

Modulation of Westerly Wind Bursts by Sea Surface Temperature: A Semistochastic Feedback for ENSO

GEOFFREY GEBBIE AND IAN EISENMAN

Department of Earth and Planetary Sciences, Harvard University, Cambridge, Massachusetts

ANDREW WITTENBERG

NOAA/Geophysical Fluid Dynamics Laboratory, Princeton University, Princeton, New Jersey

ELI TZIPERMAN

Department of Earth and Planetary Sciences, and Division of Engineering and Applied Sciences, Harvard University, Cambridge, Massachusetts

(Manuscript received 2 May 2006, in final form 26 October 2006)

ABSTRACT

Westerly wind bursts (WWBs) in the equatorial Pacific are known to play a significant role in the development of El Niño events. They have typically been treated as a purely stochastic external forcing of ENSO. Recent observations, however, show that WWB characteristics depend upon the large-scale SST field. The consequences of such a WWB modulation by SST are examined using an ocean general circulation model coupled to a statistical atmosphere model (i.e., a hybrid coupled model). An explicit WWB component is added to the model with guidance from a 23-yr observational record. The WWB parameterization scheme is constructed such that the likelihood of WWB occurrence increases as the western Pacific warm pool extends: a “semistochastic” formulation, which has both deterministic and stochastic elements. The location of the WWBs is parameterized to migrate with the edge of the warm pool. It is found that modulation of WWBs by SST strongly affects the characteristics of ENSO. In particular, coupled feedbacks between SST and WWBs may be sufficient to transfer the system from a damped regime to one with self-sustained oscillations. Modulated WWBs also play a role in the irregular timing of warm episodes and the asymmetry in the size of warm and cold events in this ENSO model. Parameterizing the modulation of WWBs by an increase of the linear air–sea coupling coefficient seems to miss important dynamical processes, and a purely stochastic representation of WWBs elicits only a weak ocean response. Based upon this evidence, it is proposed that WWBs may need to be treated as an internal part of the coupled ENSO system, and that the detailed knowledge of wind burst dynamics may be necessary to explain the characteristics of ENSO.

1. Introduction

Episodes of strong westerly winds frequently occur over the tropical Pacific (Harrison and Giese 1988; Verbickas 1998; Delcroix et al. 1993). These wind events, known as westerly wind bursts (WWBs), last for 5–40 days, and have no easterly wind analog. Although different definitions have been proposed to diagnose WWBs from observations (e.g., Harrison and Vecchi

1997; Yu et al. 2003), it is clear that every significant El Niño of the past 25 years has been accompanied by WWB activity (Kerr 1999; McPhaden 2004). WWBs cause oceanic Kelvin waves, which are directly related to subsequent warming in the eastern equatorial Pacific (e.g., Vecchi and Harrison 2000), and have been shown to play an important role in the initiation of El Niño events (Latif et al. 1988; Lengaigne et al. 2004). In this work, no distinction is made between WWBs associated with tropical cyclones, extratropical cold surges, or the Madden–Julian oscillation, and WWBs are considered at all locations in the tropical Pacific.

WWBs have typically been treated as stochastic forc-

Corresponding author address: Geoffrey Gebbie, Harvard University, 24 Oxford St., Cambridge, MA 02138.
E-mail: gebbie@fas.harvard.edu

ing in numerical models, consistent with the view that ENSO may be described as a damped oscillatory system driven by external noise (Penland and Sardeshmukh 1995; Kleeman and Moore 1997; Kessler et al. 1995; Battisti and Sarachik 1995). While WWBs occur nearly every year, numerous observational studies have shown that they are more frequent prior to and during El Niño events [see Eisenman et al. (2005), Perez et al. (2005), and Batstone and Hendon (2005) for references]. The link between the ocean state and WWBs seems to be related to movements in the western Pacific warm pool. For example, Vecchi and Harrison (2000) found that WWB occurrence is correlated with an eastward movement of the warm pool and a subsequent cooling of the far-western Pacific. Furthermore, WWBs are 3 times more likely to occur when the 29°C isotherm, a proxy for the eastern edge of the western Pacific warm pool, extends past the date line (Eisenman et al. 2005). These results imply that the ocean state affects the probability of WWB occurrence, and that WWBs do not occur in a purely random way. With this understanding, WWBs and ENSO are linked as a 2-way feedback system.

Eisenman et al. (2005) used the Zebiak and Cane (1987) model to show that, when the occurrence of WWBs is modulated by the large-scale SST pattern, there is a significant effect on the characteristics of ENSO. Given the same average number of WWBs per year, a scenario in which WWB occurrence depended upon SST resulted in an ENSO amplitude that was twice as large as in a scenario with purely stochastic WWBs. Eisenman et al. (2005) also showed that the modulation of WWBs by SST acts to destabilize the basic state, similar to the effect of an enhanced ocean–atmosphere coupling coefficient. As a result, if WWBs are included as a coupled part of the dynamics, the ocean–atmosphere system may become self-sustained and even chaotic in a parameter regime that is damped without the WWBs.

The purpose of this work is to evaluate the impact of modulation of WWBs by SST with a more complete ocean model and with a more realistic representation of WWBs than the work of Eisenman et al. (2005). Here, we use a hybrid coupled model—an ocean general circulation model coupled to a statistical atmosphere—rather than the simpler Cane–Zebiak model. The OGCM has enhanced resolution in the equatorial band and the upper ocean to reasonably represent equatorial waves and upwelling–thermocline feedbacks. Based upon an analysis of observations, the atmospheric model has been extended to explicitly account for both WWBs and the large-scale wind response. In particular,

WWBs are parameterized in a more realistic way by including two potentially important processes: a “semistochastic” trigger and the migration of WWBs along the eastern edge of the western Pacific warm pool. Semistochastic refers to WWBs that are partially modulated by the SST field and partially dependent upon stochastic processes in the atmosphere. Eisenman et al. (2005), on the other hand, modeled the extreme case where WWBs are completely determined by the warm-pool location. We find that semistochastic wind bursts are significantly more efficient at forcing interannual variability than purely stochastic wind bursts. A number of investigators (e.g., Picaut et al. 1997) have hypothesized the importance of SST advection by zonal surface currents at the warm-pool edge. The more extensive and realistic representation of WWBs leads to results that agree with Eisenman et al. (2005) in some respects, such as the fact that the modulation of WWBs can transfer the system into self-sustained oscillations; but here we show that WWBs cannot be parameterized by simply increasing the linear air–sea coupling coefficient of wind stress and SST.

A description of the hybrid coupled model used here, our representation of the WWBs, and their triggering mechanism is provided in section 2. We then explore the effects of WWB modulation by the SST in the deterministic and semistochastic limits, and we compare these results with the case in which WWBs are assumed to be purely stochastic in section 3. The impact of WWBs on the characteristics of ENSO, such as amplitude, period, and asymmetry, are discussed in section 4. Section 5 provides a summary of our results and the implications for future studies.

2. The hybrid coupled model, WWB characteristics, and WWB parameterization

The hybrid coupled model used here is based upon the Geophysical Fluid Dynamics Laboratory (GFDL) Modular Ocean Model version 4 (MOM4; Griffies et al. 2003) coupled to a linear statistical atmosphere, as described by Harrison et al. (2002), Wittenberg (2002), and Zhang et al. (2005). The ocean model has a global domain and enhanced resolution in the Tropics ($1/2^\circ$ meridional resolution, 2° zonal resolution). The meridional resolution becomes coarse in the extratropics (e.g., 4° at 50°N). The model includes an explicit free surface with explicit freshwater surface fluxes (Griffies et al. 2001), a neutral physics package (Gent and McWilliams 1990), and the *K*-profile parameterization (KPP) ocean mixing scheme (Large et al. 1994). Penetration of short-wave radiation into the surface layers is parameterized in terms of ocean color (Sweeney et al. 2005). The at-

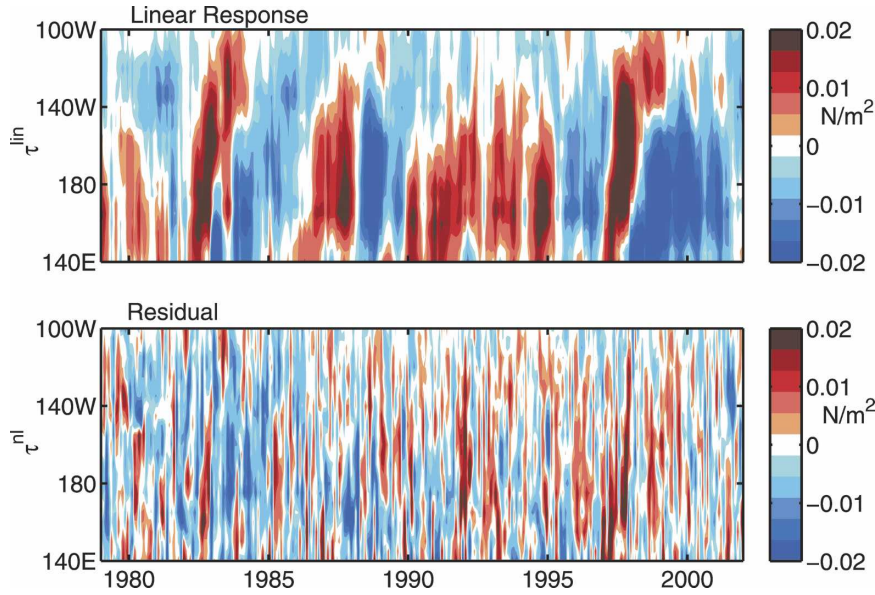


FIG. 1. Decomposition of the ERA-40 zonal wind stress anomaly, 1979–2002, into two components: (top) the part explained by the first seven singular vectors that maximize SST–wind stress covariance (linear response) and (bottom) the residual. Both (top) and (bottom) are time–longitude sections with wind stress averaged from 5°N to 5°S. The maximum wind stress anomalies are approximately 0.03 N m⁻² for both the linear response and residual components. Color scales for all figures are ±0.02 N m⁻².

mosphere model includes both a linear statistical component and a WWB component (to be detailed in the following).

a. Statistical atmosphere model

The statistical atmosphere is constructed from the 40-yr European Centre for Medium-Range Weather Forecasts (ECMWF) Re-Analysis (ERA-40) wind stress and SST from 1979 to 2002 in the tropical Pacific (20°N–20°S and 120°E–70°W). A singular value decomposition (SVD; Neelin 1990; Bretherton et al. 1992; Roulston and Neelin 2000) is performed on the monthly mean SST and wind stress anomaly covariance matrix. The leading seven SST singular vectors consist of basin-scale patterns of SST anomalies, which covary strongly with the observed wind stress anomalies. Following Wittenberg (2002), the observed zonal wind stress anomalies at each spatial point are regressed onto the leading SST singular vectors.

To evaluate how well the statistical atmosphere describes the observational record, the wind stress anomalies can be reconstructed from the observed SST. The reconstructed wind stress is called the linear-response wind, τ^{lin} . The zonal wind stress can then be decomposed into three parts:

$$\tau_x = \bar{\tau} + \tau^{\text{lin}} + \tau^{\text{nl}}, \quad (1)$$

where $\bar{\tau}$ is the seasonal climatology and τ^{nl} is a residual not linearly related to SST (Fig. 1). The first seven SVD modes explain 98.6% of the covariance between the SST and zonal wind stress. About 90% of the SST variance and 55% of the wind stress variance in the equatorial band (5°N–5°S) is captured.

A baseline coupled model state is constructed in two steps. First, the coupled model is spun up with restoring to observed SST and sea surface salinity (SSS). The ocean is forced by the climatological monthly winds, to which the atmosphere model adds the linearly coupled wind stress anomalies. Second, the bias between the seasonal steady state and the observed SST and SSS seasonal climatologies is calculated. The model is again run to a steady state with corrected restoring surface fields to minimize the bias. The resulting model climatology is constrained to be very close to the observations through the adjustment of the surface net heat flux and freshwater flux. The remaining biases include a thermocline that is slightly too shallow and too diffuse [for a full description of the model climatology obtained with this procedure, see Harrison et al. (2002) and Wittenberg (2002)].

When the linear statistical atmosphere is coupled to the OGCM, the resulting system is stable with a decay time scale of 3 yr (Fig. 2). The coupling coefficient between wind stress and SST is determined by linear re-

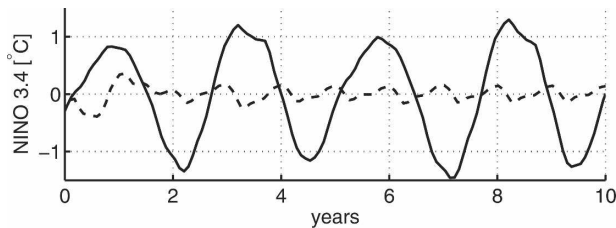


FIG. 2. Niño-3.4 index of numerical simulations with an ocean general circulation model coupled to a linear statistical atmosphere with empirically determined air-sea coupling coefficients (dashed) and with coefficient artificially increased by 50%.

gression, and hence, has an empirical value. To more fully understand the dynamical regime of the baseline system, the coupling coefficient can be artificially increased. When the coefficient is 1.5 times the empirical value, self-sustained regular oscillations are present (Fig. 2).

The statistical model is an annually averaged one, which is known to reduce the instability of the coupled ocean-atmosphere system (e.g., Tziperman et al. 1995), and therefore the stability regime of ENSO cannot be reliably estimated when using this representation of the atmosphere. Stable coupled ocean-atmosphere models have been shown to describe ENSO well (e.g., Battisti and Sarachik 1995; Penland and Sardeshmukh 1995; Kleeman and Moore 1997), and this regime is the appropriate one for studying whether WWBs modulated by the ocean state can render the basic state unstable. In the case that the ocean-atmosphere system without WWBs is already unstable, WWBs will necessarily have a less dramatic effect (to be discussed more fully later in this paper).

b. WWB characteristics

The aforementioned linear statistical atmosphere does not explicitly deal with WWBs. A first question is whether a part of the WWB signal is captured by the statistical atmosphere model. To answer this question, we must first define the WWBs. A number of different criteria have been used in the literature to identify WWBs, and here we will explore two definitions: 1) all instances of westerly wind speed anomalies above 7 m s^{-1} and sustained above 4 m s^{-1} for 5 or more days (Eisenman et al. 2005), and 2) all zonal wind anomalies above 4 m s^{-1} . Both definitions define the anomaly to be relative to the seasonal climatology.

Definition 1 identifies 84 WWBs during 1979–2002, or an average of 3.6 WWBs per year. The composite WWB has a roughly Gaussian shape in both space and time, although observed tails in the spatial structure are generally smaller than those of a Gaussian. By fitting a

Gaussian to the composite WWB by the method of least squares, we find an estimate for the magnitude, length and time scale of WWBs. If the WWB zonal wind stress is expressed as

$$\tau_{\text{WWB}}(x, y, t) = M \exp \left[-\frac{(t - t_o)^2}{T^2} - \frac{(x - x_o)^2}{X^2} - \frac{(y - y_o)^2}{Y^2} \right], \quad (2)$$

where (x_o, y_o) are the center longitude and latitude of the WWB, and t_o is the time of peak wind, we find that $M = 0.07 \text{ N m}^{-2}$, $X = 20^\circ$ longitude, $Y = 6^\circ$ latitude, and $T = 5$ days. (The spatial structure of a modeled WWB is given in the top panel of Fig. 5.) Our findings are similar to those of Harrison and Vecchi (1997) for the 1986–1995 period. Of particular importance is the strength of the composite WWB. The wind measure of the composite, defined as the time integral of the average WWB wind speed, is $1.1 \times 10^6 \text{ m}$ [cf. to $1.0\text{--}1.5 \times 10^6 \text{ m}$ of Harrison and Vecchi (1997)]. Another measure of the strength of a WWB is obtained by integrating the WWB zonal wind stress over space and time: the composite WWB imparts an impulse (momentum input) of 145 PN s (petanewton seconds).

Definition 1, like other WWB definitions in the literature, is somewhat arbitrary. To minimize the arbitrariness, we also use definition 2 to identify WWBs: all anomalous westerlies greater than 4 m s^{-1} . Using this definition, many WWBs cannot be distinguished as individual events. The net westward stress of definition 2 between 5°N and 5°S is 510 PN s yr^{-1} , nearly equivalent to the wind stress imparted by 3.6 WWBs yr^{-1} in the first definition. Definition 2 will be used for the remainder of this paper because of its simplicity.

Previously, the wind stress field was decomposed without regard to WWBs; we now explicitly account for WWBs when decomposing the wind. The new decomposition includes the WWBs, τ_{WWB} , and the non-WWB wind field, τ_* , so that the total wind field is $\tau_x = \tau_{\text{WWB}} + \tau_*$. The diagnosed WWBs in the ERA-40 wind stress field are plotted in the top panel of Fig. 3. The non-WWB field is then split into a seasonally varying climatology and a residual, $\tau_* = \overline{\tau_*} + \tau_*'$. Next, a linear statistical model is derived using SVD and the linear regression method of section 2a. Now the non-WWB wind anomaly field, τ_*' , is decomposed into the linearly explained part, $\tau_*'^{\text{lin}}$, and the part that is not linearly related to SST, $\tau_*'^{\text{nl}}$ (middle and bottom panels, Fig. 3). Putting everything together, the total wind stress field has four parts:

$$\tau_x = \tau_{\text{WWB}} + \overline{\tau_*} + \tau_*'^{\text{lin}} + \tau_*'^{\text{nl}}. \quad (3)$$

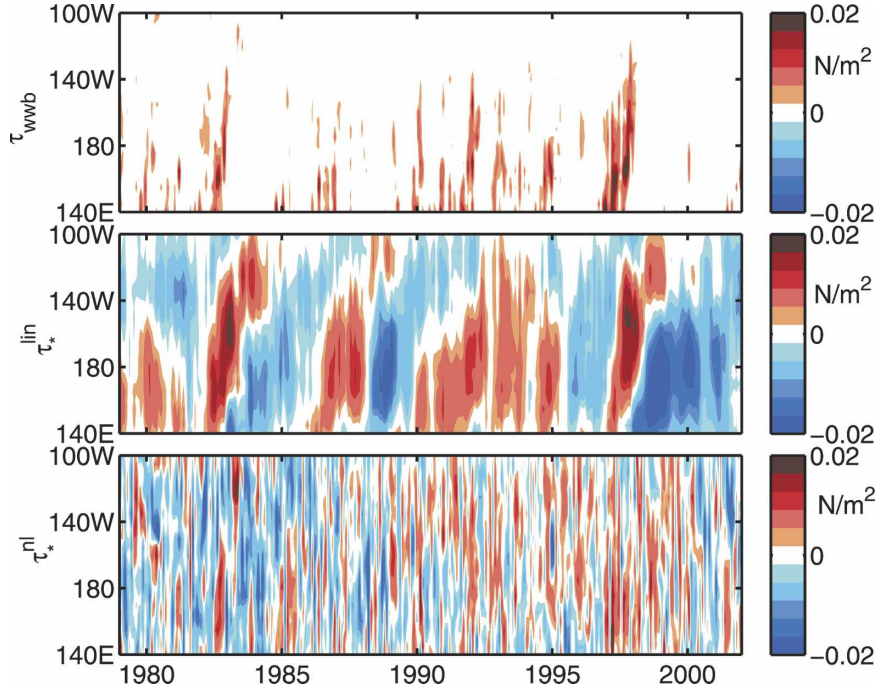


FIG. 3. Decomposition of the ERA-40 zonal wind stress anomaly, 1979–2002, into three components using the same format as in Fig. 1. (top) The WWB component of the winds. (middle) The non-WWB part of the wind stress is explained by the first seven singular vectors of an SVD analysis of the SST–wind stress covariance matrix. (bottom) The residual winds that are neither classified as a WWB nor explainable in the SVD analysis.

How much of the WWB activity is a linear response to SST? Subtracting Eq. (3) from Eq. (1), the following relation results:

$$\tau_{\text{WWB}} = (\bar{\tau} - \bar{\tau}_*) + (\tau_*^{\text{lin}} - \tau_*^{\text{lin}}) + (\tau_*^{\text{nl}} - \tau_*^{\text{nl}}). \quad (4)$$

Term 1 on the right-hand side is the seasonal climatology of WWBs, term 2 is the part of the WWBs explained by the standard linear atmosphere of the previous section, and term 3 is the part that is not a linear response to SST.

For the ERA-40 observations of 1979–2002, the relative importance of the three terms can be evaluated. In the equatorial band, the three terms account for 11%, 39%, and 50% of the total WWB impulse, respectively. To better illustrate these results, consider the strong WWB activity in 1997. Figure 4 shows the part of WWBs explained by the climatology and a linear response to the SST (middle), and the part that cannot be linearly related (bottom). About 45% of the total impulse during 1997 would not be explained by a standard linear statistical atmosphere. As will be shown in section 3, this part of the WWBs can be important in determining the dynamical regime of ENSO.

c. WWB parameterization

To build a modified atmospheric component to the coupled model, we use Eq. (3) as a guide. The seasonal climatology of wind stress is imposed upon the ocean, and the linear-response wind is calculated based on the SST anomaly. Next, a new parameterization must be developed to predict the WWB component of the wind stress. Finally, there is a portion of the wind stress, τ_*^{nl} , which is not modeled here, but is sometimes modeled as a random process.

The goal of WWB parameterization in this study is not to predict the exact details of individual WWBs, but rather to represent the general dependence of WWB characteristics on the SST in a simple way while capturing the essence of the observations. To accomplish this, we parameterize the observed relation between the extended warm pool and WWB occurrence (Fig. 5). The warm-pool edge, x_{pool} , is defined to be the location of 29.0°C isotherm. The center of the WWB is chosen to be 15° west of the warm-pool edge, $x_o = x_{\text{pool}} - 15^\circ$, in agreement with observations. We choose to focus on WWBs at the equator, $y_o = 0$, although off-equator WWBs may be dynamically important as well (Harrison and Vecchi 1999). For consistency, the total west-

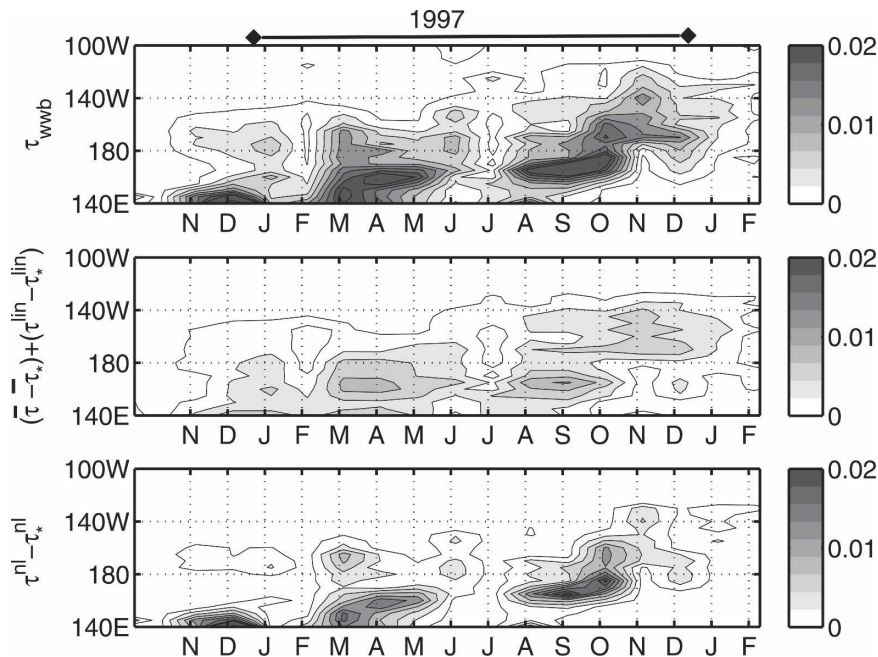


FIG. 4. (top) Average zonal wind stress over 5°N to 5°S due to WWBs, τ_{WWB} . (middle) Part of the WWB zonal wind stress explained by the seasonal climatology and a linear response to SST, $(\bar{\tau} - \bar{\tau}_*) + (\tau^{\text{lin}} - \tau_*^{\text{lin}})$. (bottom) Part of WWB zonal wind stress unexplained by a linear response to SST, $(\tau^{\text{nl}} - \tau_*^{\text{nl}})$.

erly stress of parameterized equatorial WWBs is tuned to be equal to the amount of WWB stress observed between 5°N and 5°S .

Next, we describe specifically how WWBs are triggered in our model. We use three variants of this trigger: deterministic, semistochastic, and purely stochastic. In the deterministic case, a WWB is triggered whenever the warm pool extends past the date line. The atmospheric time step is 1 day, so the criterion is checked once per day. In the purely stochastic case, WWBs are triggered randomly (their probability of occurrence is constant through time, $P = P_o$). The deterministic and purely stochastic triggers may be thought of as two unrealistic limiting cases. In the semistochastic case, the probability of WWB occurrence depends upon the extent of the warm pool (bottom panel of Fig. 5),

$$P = P(x_{\text{pool}}) = \frac{P_o}{2} \times \left\{ \tanh \left[\frac{(x_{\text{pool}} - 180)\pi}{40.0} \right] + 1.0 \right\}. \quad (5)$$

This functional form is meant as a simple parameterization of the observed increased probability of WWB occurrence with increased warm-pool extent (Yu et al. 2003).

WWBs are most common in boreal winter, as seen in Fig. 23 of Harrison and Vecchi (1997). To crudely pa-

rameterize this effect, most model integrations here do not allow WWBs in boreal summer (July, August, September), that is, $P = 0$ in the summer. The sensitivity of our results to the assumed seasonal structure of WWB occurrence will be revisited in section 4.

In the model, each WWB starts at a triggering time, t_{init} , builds up to full strength at $t = t_o$, and finally decays. Two additional parameters are needed to fully describe this WWB evolution. The parameter $t_{o-\text{init}}$ is the time between the triggering of the event t_{init} and its peak t_o . For a smooth increase of wind stress with time, $t_{o-\text{init}}$ should be slightly larger than T in (2). Observations show that it is not common to have two simultaneous WWBs, so only one WWB is allowed at a time for simplicity. Consequently, a final necessary parameter is t_r , the minimum interval between WWBs. The probability distribution function of observed t_r , taken as the separation time between WWBs (not shown), has a mode at 15 days, but median at 30 days and mean at 40 days. It is not clear which value of t_r is most relevant, so the sensitivity to this choice is investigated later. A full list of model parameters and their values are given in Table 1.

3. Impact of ocean modulation of WWBs

To understand the impact of WWBs on ENSO dynamics, this section is split into three parts. In section

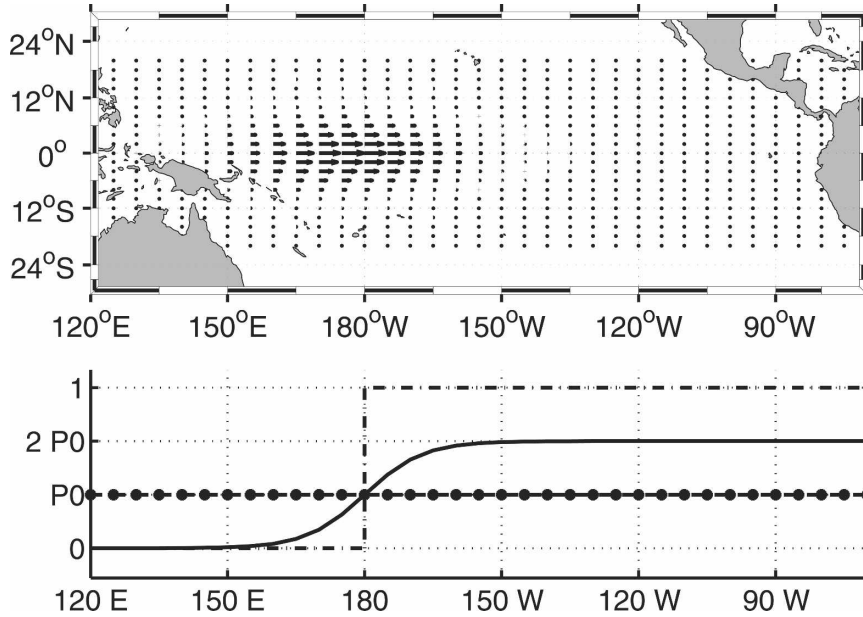


FIG. 5. (top) Spatial form of the modeled WWB. Vectors represent the anomalous wind stress with a maximum value given in Table 1. This is a representative snap shot of a WWB; in the prognostic model, the central longitude of different WWBs varies depending on the longitude of the warm-pool edge. (bottom) Probability of triggering a WWB as a function of longitudinal warm-pool extent. In the numerical experiments described here WWBs are triggered with one of three probability functions: 1) deterministic WWBs (dashed-dotted line), 2) semistochastic WWBs (solid line), and 3) purely stochastic WWBs (solid dotted line). Note that the y axis is not drawn to scale.

3a, we examine the impact of modulated WWBs on the long-term ENSO statistics. For this purpose, we consider the three previously mentioned scenarios for adding WWBs to the model: WWBs that are purely stochastic, WWBs triggered by the warm-pool extent in a deterministic way, and the more realistic scenario in which the WWBs are semistochastically triggered. In section 3b, the effect of parameterized WWBs on a composite modeled El Niño event is analyzed. In section 3c, we investigate the effect of the eastward migration of WWBs during a warm event.

a. Sensitivity to WWB trigger

How is the ENSO cycle affected by modulated WWBs over interannual and decadal time periods? A 25-yr model integration with deterministically triggered and migrating WWBs is shown in Fig. 6. The modulated WWBs lead to interannual ENSO variability with a Niño-3.4 (5°N–5°S, 170°–120°W) standard deviation of 0.7°C. It is important to note that there is no external forcing in this run, and that without WWBs the model decays to the seasonal cycle. Yet, with the deterministically triggered WWBs, interannual variability is self-sustained. There are 3.5 WWBs yr⁻¹ on average in this

run, roughly equivalent to the 3.6 WWBs yr⁻¹ that were found in the observations.

Figure 6 shows oscillations at periods of 2 and 3 yr with deterministic WWBs. Both the magnitude and period of ENSO are sensitive to the details of the WWB formulation. When the WWB recurrence interval (t_r in Table 1) is decreased from 25 to 15 days, the period

TABLE 1. Modeled westerly wind burst parameters. The default values of the parameters are given here, and in the case that any parameter is changed, it will be explicitly mentioned in the text. Here x_{pool} is the warm-pool extent in degrees longitude defined by the warm-pool temperature θ_{pool} .

WWB parameter	Symbol	Value
Magnitude	M	0.07 N m ⁻²
Zonal width	X	20°
Meridional width	Y	6°
Duration	T	5 days
Center longitude	x_o	$x_{\text{pool}} - 15^\circ$
Center latitude	y_o	0° (equator)
Peak-wind time	t_o	$t_{\text{init}} + t_{o-\text{init}}$
Peak response time	$t_{o-\text{init}}$	12.5 days
Recurrence interval	t_r	25 days
Warm-pool-edge SST	θ_{pool}	29.0°C
WWB probability day ⁻¹	P_o	0.05 day ⁻¹

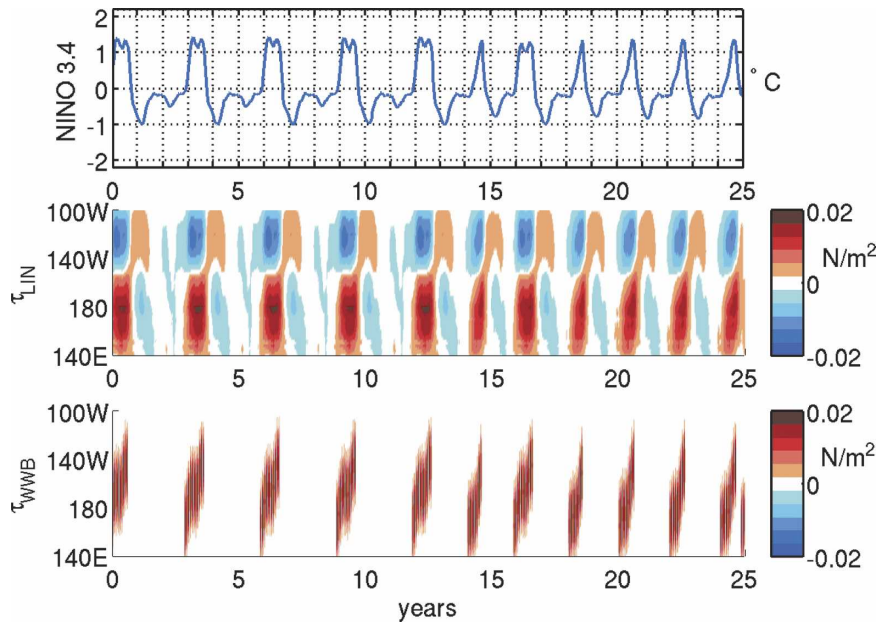


FIG. 6. A 25-yr window of an integration of the hybrid coupled model with WWBs triggered deterministically with the parameters of Table 1. (top) A time series of the Niño-3.4 index. (middle) A time–longitude section of zonal wind stress anomaly, $\tau_{\text{LIN}}^{\text{lin}}$, of the linear statistical atmosphere, averaged between 5°N and 5°S . (bottom) A time–longitude section of zonal wind stress anomaly caused by WWBs.

increases to 4 yr and the standard deviation of Niño-3.4 increases to 0.8°C . An experiment with a longer recurrence time, that is, $t_r = 40$ days, has the opposite effect [$\text{std}(\text{Niño-3.4}) = 0.61$, with El Niño recurrence intervals of 2 and 3 yr]. The focus of this study is not to show that one particular set of WWB parameters is quantitatively superior. Instead, we emphasize the qualitative message that the addition of deterministic coupled WWBs of realistic strength leads to a new self-sustained oscillating regime in all explored cases.

We now move to the similarly extreme and unrealistic scenario in which the WWBs are purely stochastic. In this case, WWBs occur independently of the ocean state (Fig. 7), and the probability of their occurrence, P_o , is tuned to 0.0205 day^{-1} so that there are 3.6 WWBs yr^{-1} , as observed. The standard deviation of Niño-3.4 is only 0.2°C , much less than the deterministic case despite the fact that there is the same average number of WWBs per year.

A semistochastic model allows for some stochasticity in the time of WWB occurrence such that they are more likely to occur when the warm pool extends [Eq. (5)]. A run with semistochastic WWBs is shown in Fig. 8 (hereafter referred to as semistochastic run 1). With model parameters $t_{o\text{-init}} = 7.5$ days, $t_r = 15.0$ days, and $P_o = 0.042 \text{ day}^{-1}$, the model produces an average of 3.6 WWBs yr^{-1} over a 100-yr interval. The Niño-3.4 standard deviation is now 0.5°C , significantly larger than

the purely stochastic case. The recurrence interval of El Niño events is 2–5 yr. Figure 8 shows that WWBs occur in groups of 3–8, much like in observations. These results are generally consistent with those of Eisenman et al. (2005) using the simpler Cane–Zebiak model without the semistochastic treatment: the modulation of the WWBs by the large-scale SST structure critically affects the resulting ENSO amplitude.

It should be added that the interannual variability of the semistochastic runs can be tuned to obtain a range of results. With model parameters $t_{o\text{-init}} = 12.5$ days, $t_r = 25.0$ days, and $P_o = 0.05 \text{ day}^{-1}$, there are 3.7 WWBs yr^{-1} and a Niño-3.4 standard deviation of 0.3°C (semistochastic run 2, not shown). It appears, in any case, that the semistochastic ENSO response, as measured by the Niño-3.4 variance, is bounded by the purely stochastic and deterministic cases.

b. The effect of parameterized WWBs on the evolution of an El Niño event

The previous results show that WWBs can change the magnitude of interannual variability, but it remains to be explained how the wind bursts accomplish this, and why different wind burst formulations lead to different results. The evolution of a composite warm episode in semistochastic run 1 is plotted in Fig. 9. As soon as summer ends, the warm pool expands eastward and WWBs occur and cause rapid warming in the central

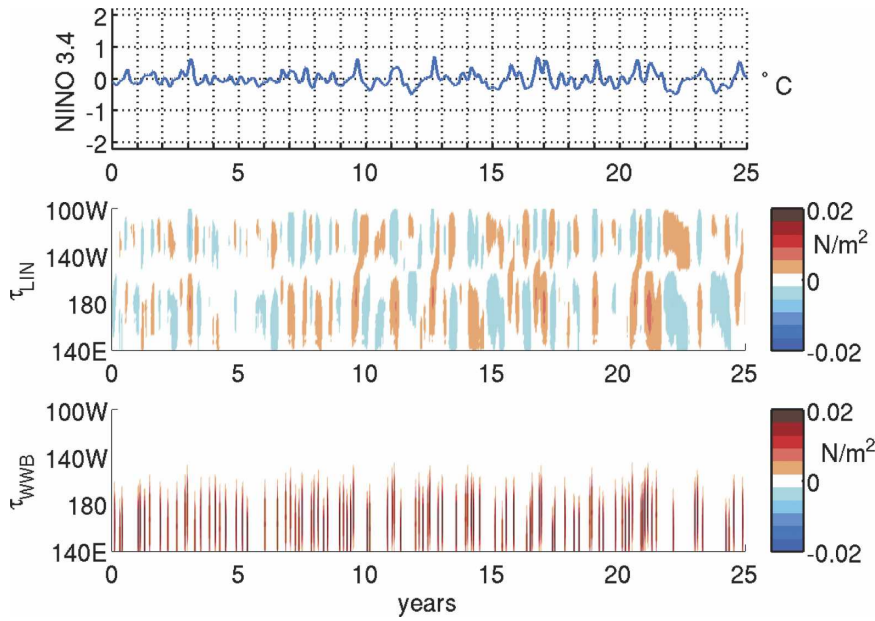


FIG. 7. Same as in Fig. 6, except for WWBs triggered in a purely stochastic way.

Pacific. Note that the WWBs are strong enough to reverse the direction of the trade winds. It will be shown below that WWB-forced oceanic Kelvin waves lead to the warming in the central and eastern Pacific, as seen in observations (Harrison and Schopf 1984). In the composite, east Pacific warm events peak between January and March, consistent with the known phase locking of ENSO. However, the SST anomalies do not extend to the South American coast as seen in observed record, a common model bias.

The rapid growth of the modeled El Niño in autumn is similar to the timing of the 1986 El Niño, but unlike the large events of 1982 and 1997. Our stipulation of no WWBs in summer is critical in setting up the onset timing. From this limited evidence, it appears that the seasonal cycle of WWBs may have a role in the seasonal phase locking of ENSO. An improved understanding of the link between WWBs and the seasonal cycle therefore deserves further study, but is beyond the scope of this work.

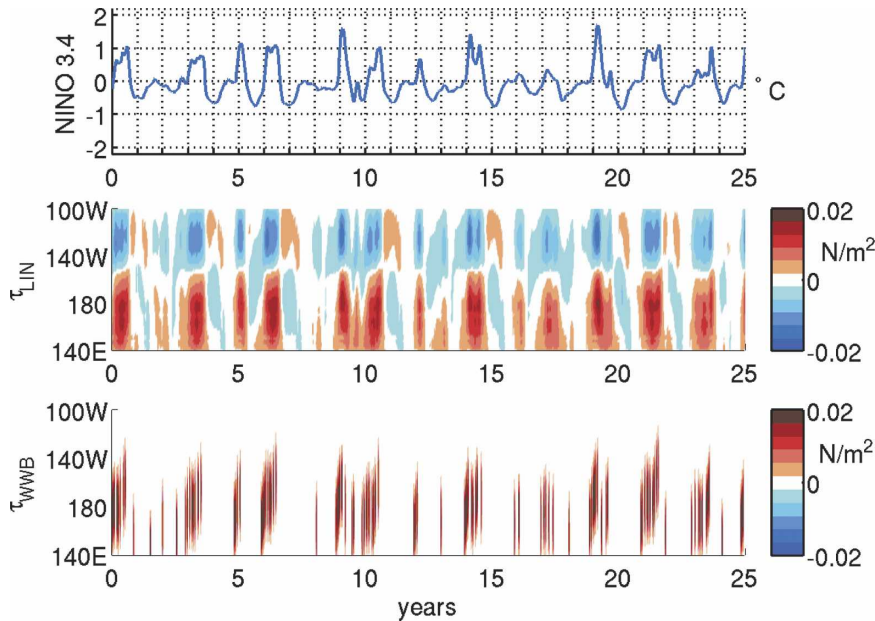


FIG. 8. Same as in Fig. 6 and Fig. 7, except for WWBs triggered in a semistochastic way.

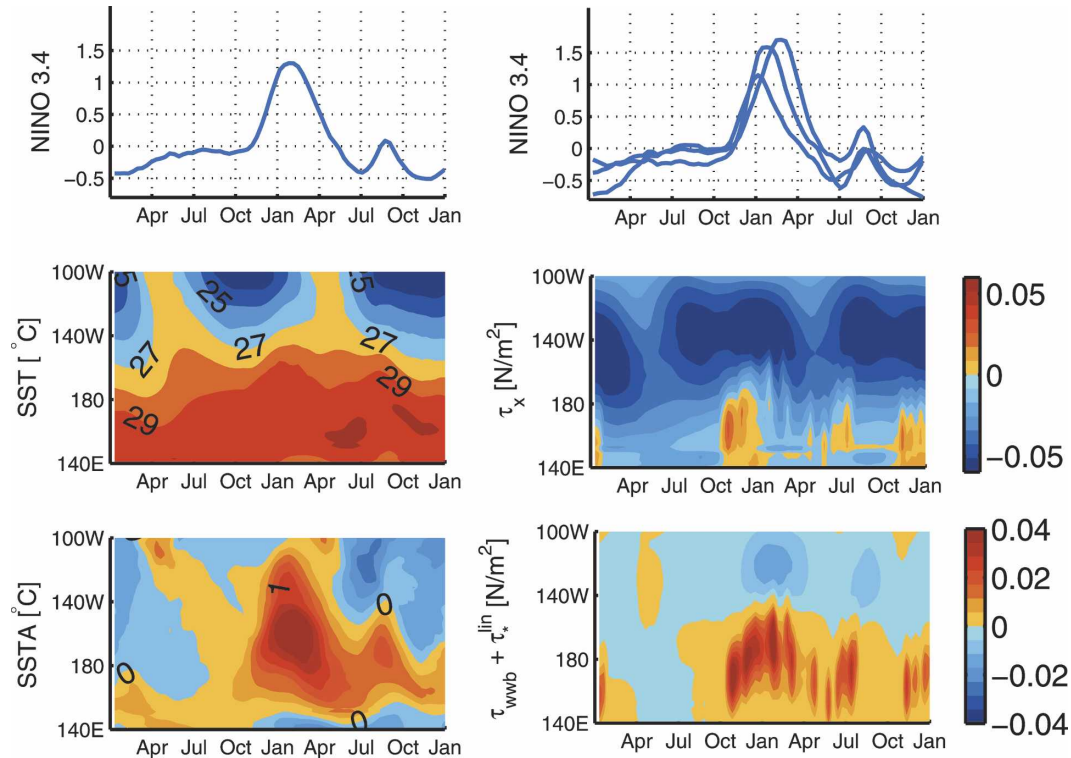


FIG. 9. A composite warm episode in the semistochastic model simulation. (top left) Composite Niño-3.4 index derived from (top right) three individual warm episodes. (middle left) Time-longitude plot of SST and (middle right) total zonal wind stress. (bottom) Same as in (middle), but for (left) SST anomaly relative to the seasonal climatology, and (right) the zonal wind stress simulated from the linear statistical model and the WWB model. The contour intervals are: 1°C for SST, 0.01 N m^{-2} for total zonal wind stress, 0.25°C for SST anomaly, and 0.005 N m^{-2} for zonal wind stress anomaly.

To determine whether the high-frequency component of WWBs is important, we take a 7-yr run from the deterministic WWB model and low-pass filter the wind field with a 4-month running mean at each point in space. The filtering is done “off-line,” and then the smoothed wind stress time series is used to force the simulation. In this way, the impact of the full WWBs is compared to that of the smoothed WWBs. We find that the ENSO cycle is hardly affected (Fig. 10) and that the slow component of WWBs is most important for determining the ENSO response. The results imply that the nonlinear transfer of energy from high frequency to low frequency is small. Roulston and Neelin (2000) and Eisenman et al. (2005) found similar results with intermediate complexity models, even though the OGCM of this study includes more ocean processes at higher resolution allowing for more nonlinear effects. Latent heat and evaporation feedbacks are not explicitly included in the atmosphere model here, and thus their ability to rectify high-frequency variability into low frequencies cannot be ascertained (cf. Kessler and Kleeman 2000).

Although the input of total stress was equivalent for the three types of WWB triggers, the variance of the Niño-3.4 index in the interannual band was sensitive to the trigger type. For deterministically triggered WWBs, a large component of the WWBs projects into the interannual band because of the modulation by SST. For stochastically triggered WWBs, the frequency spectrum is white and there is a much smaller projection into the interannual band. In the model, WWB modulation by SST enhances the slowly varying component of WWBs, and hence enhancing the modeled interannual ENSO variability as well. The projection of WWB energy into interannual frequencies is nearly linearly related to the interannual ENSO variability, and the range of behavior with different WWB triggers is explained.

c. Role of WWB migration

WWBs are observed to migrate eastward during El Niño events. Our parameterized WWB events allow us to examine the role of this migration in the dynamics of ENSO. Consider three model runs with identical initial conditions from the spinup run. Without WWBs, the

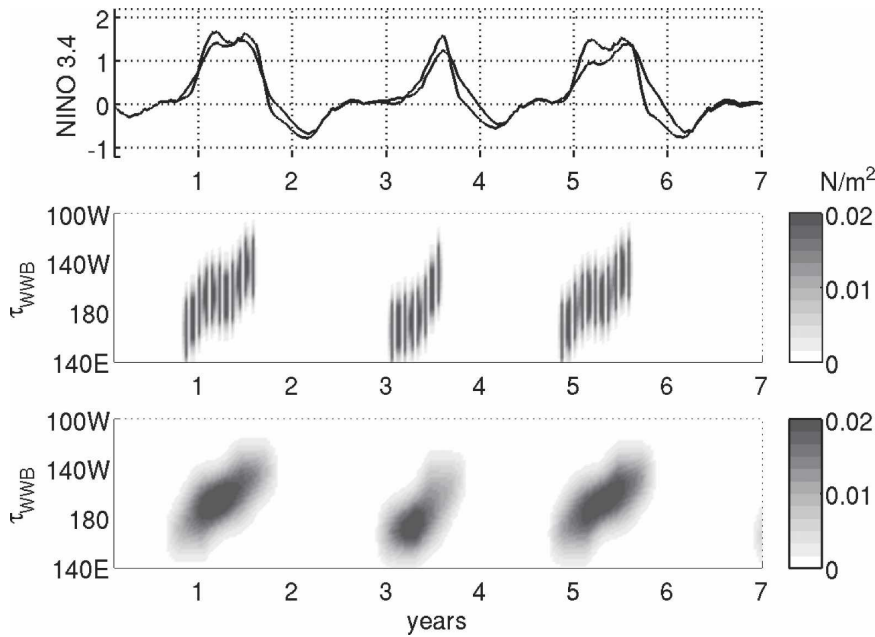


FIG. 10. A comparison of the hybrid coupled model when forced by two wind fields with nearly identical low-frequency energy. (top) Time series of Niño-3.4 index for the two model runs (to be distinguished below). (middle) A time–longitude section of the WWB part of the zonal wind stress anomaly in run 1, corresponding to the Niño-3.4 index with slightly greater excursions away from zero. (bottom) A time–longitude section of imposed zonal wind stress anomaly in run 2, corresponding to the Niño-3.4 index with slightly smaller excursions and a small time lag behind the first index. The imposed wind stress anomaly is the WWB field of run 1 with a 4-month running mean.

model is stable such that all perturbations eventually decay to the seasonal cycle (dashed line, top panel of Fig. 11). The second run uses deterministically triggered WWBs and the parameters of Table 1 but with constant central longitude, $x_o = 170^\circ\text{E}$ (see right column, Fig. 11). In the third run, we maintain the deterministic trigger but allow the WWBs to occur at different longitudes following the edge of the warm pool, as in section 3a. An individual WWB does not migrate, but subsequent WWBs may occur at different longitudes. In runs 2 and 3, WWBs commence in October, the warm pool extends, and WWBs migrate eastward in the following months (right column, Fig. 11). Rapid warming of the eastern tropical Pacific through Kelvin waves is seen in the vertical velocity field at the depth of the thermocline. The bottom panels of Fig. 11 show the difference in vertical velocity between a WWB run and the non-WWB run (run 1), clearly isolating the impact of the wind bursts. The east Pacific warm anomaly is maintained until the early summer by continued WWBs. In both runs 2 and 3, therefore, WWBs trigger and amplify the El Niño event.

The onset of the warm event is more rapid in the case with migrating WWBs. Also, the peak Niño-3.4 index is 0.4°C greater in January. WWB migration enables a

new coupled feedback: WWBs not only force Kelvin waves but also enhance the eastward advection of the warm-pool edge (e.g., Picaut et al. 1997; Lengaigne et al. 2004). This feedback is not active in the nonmigrating case because the zonal velocity anomaly is not collocated with the SST anomaly a few months after the onset of the warm event. The warm pool–advection feedback in our model differs in some important ways from the study of Lengaigne et al. (2004). Here, latent heat and evaporation feedbacks are not included, and Lengaigne et al. (2004) showed that these feedbacks lead to a maximum zonal current anomaly on the eastern edge of the SST anomaly in their model, a favorable situation for increased zonal advection of SST. In our model, the maximum current anomaly is collocated with the maximum SST anomaly (SSTA), not the maximum SSTA gradient, and therefore our estimate of the strength of the warm pool–advective feedback is probably an underestimate.

4. Discussion

Modulation of westerly wind bursts by the SST strongly affects the amplitude of interannual variability in our model. The Niño-3.4 standard deviation in 100-yr model runs with different WWB representations is

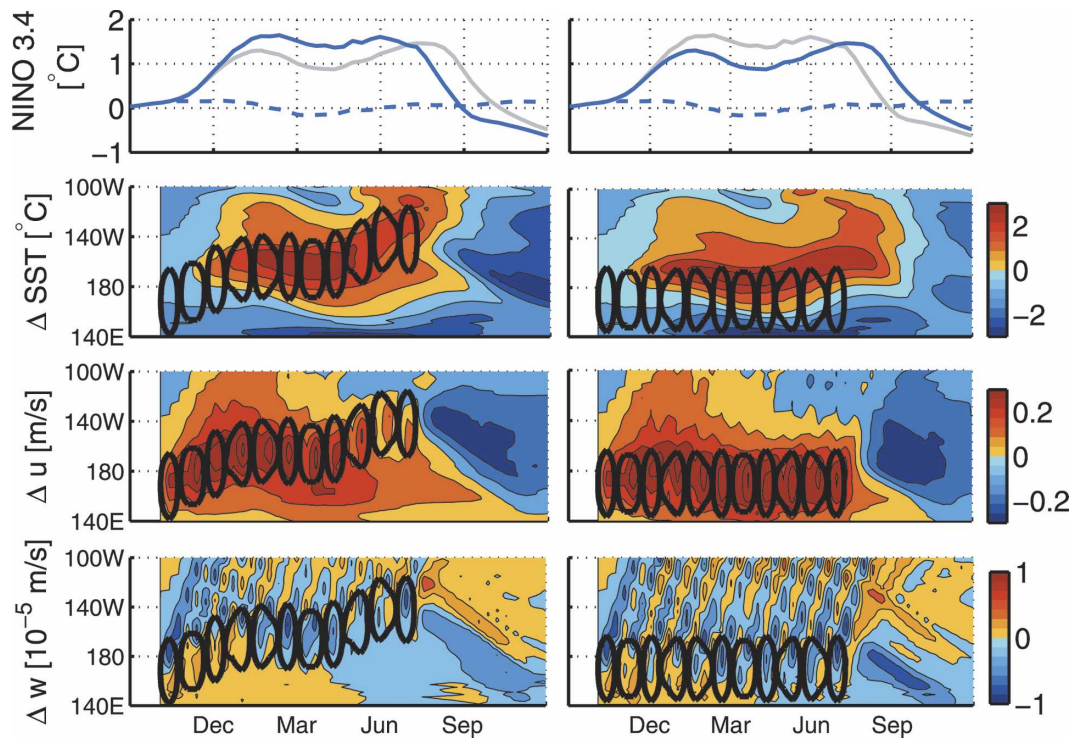


FIG. 11. Comparison of a simulated warm episode with WWBs migrating with (left column) the warm-pool edge, and (right column) WWBs at a fixed location. (top) Niño-3.4 index for the migrating WWB case (blue line in left column and gray line in right column); the fixed WWB case (gray in left column and blue in right column); and the no-WWB case (blue dashed line). (second row) Time-longitude section of SST difference between WWB run and no-WWB run. (third row) Difference in zonal velocity between WWB run and no-WWB run. (bottom row) Difference in vertical velocity at the depth of the thermocline. All quantities are averaged from 5°N to 5°S and averaged over 10-day intervals. WWBs are indicated by the bold black lines.

summarized in Table 2. As seen in section 3, deterministically triggered WWBs are most effective at producing interannual variability [$\text{std}(\text{Niño-3.4}) \approx 0.7^{\circ}\text{C}$] and purely stochastic WWBs produce weaker interannual variability [$\text{std}(\text{Niño-3.4}) \approx 0.2^{\circ}\text{C}$]. Semistochastic WWBs produce interannual variability between these two limiting cases [$\text{std}(\text{Niño-3.4}) \approx 0.3\text{--}0.5^{\circ}\text{C}$]. Semistochastic and deterministic WWBs consistently generate a more energetic ENSO cycle because of the enhancement of the slow component of the WWBs, which is caused by the WWB modulation by the SST.

The model runs in section 3 used two components of the coupled atmosphere: the linear-response winds and the WWB parameterization. A remaining significant component is the residual wind field, τ_{*}^{nl} ($\approx 30\%$ of the domain-integrated wind stress variance; see section 2). When adding the residual winds to the model forcing, the standard deviation of Niño-3.4 is increased by about 0.2°C in all cases. This does not change our main results: semistochastic WWBs lead to significantly larger interannual variability than purely stochastic WWBs.

TABLE 2. WWB experiments and the variable WWB parameters. Here $t_{o\text{-init}}$ is the time between the WWB trigger and peak wind, t_r is the minimum time interval between WWBs, and P_o is the probability of triggering a WWB at each model time step ($\Delta t = 1$ day). The average number of WWBs per year is tuned to be near 3.6. The final column displays the standard deviation of the Niño-3.4 index over a 100-yr model run.

Experiment	$t_{o\text{-init}}$ (days)	t_r (days)	P_o (day^{-1})	WWBs yr^{-1}	$\text{std}(3.4)^{\circ}\text{C}$
Deterministic	12.5	25	—	3.52	0.68
Semistochastic 1	7.5	15	0.042	3.64	0.51
Semistochastic 2	12.5	25	0.050	3.72	0.33
Stochastic	12.5	25	0.0205	3.62	0.22

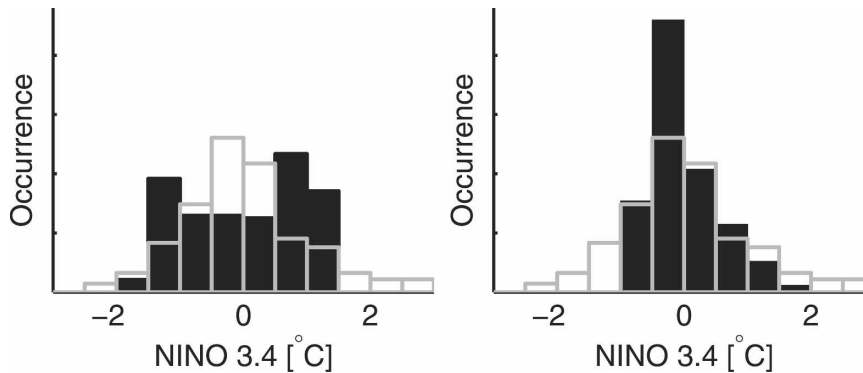


FIG. 12. Normalized histograms of the Niño-3.4 index from observations (gray bars), from (left) the coupled model simulation with artificially increased air-sea coupling coefficients (black histogram), and (right) semistochastic run 1 (black histogram).

At this point we may be in a position to discuss the origin of irregularity of ENSO. The ENSO cycle with deterministic WWBs shifts from 2- to 3-yr periods at irregular times. The modeled ENSO irregularity is likely the result of low-order deterministic chaos (Tziperman et al. 1994, 1995; Jin et al. 1994). However, the overall character of the oscillation seems more regular than observed. The characteristics of ENSO are sensitive to the details of the WWB formulation, so it is difficult to rule out the possibility that the deterministic system produces even more irregular behavior with a different model formulation. For example, our formulation restricted WWBs to the equator. Allowing for off-equatorial WWBs determined by an asymmetric SST distribution about the equator may make the model ENSO more irregular.

The probability distribution function (PDF) of the observed Niño-3.4 SSTA is asymmetric, indicating larger warm events than cold events (e.g., Perez et al. 2005). This asymmetry occurs in most models because of the vertical advection term in the SST equation and the nonlinearity of the mean temperature versus depth profile (Battisti 1988). The timing of WWBs seems to be an important factor here. They occur during the growth phase of warm events, and therefore growth of SST anomalies is enhanced during these times. As a result, the hybrid coupled model with WWBs produces PDFs that are skewed positively, while our runs without WWBs have more symmetric distributions (see Fig. 12). This evidence suggests that WWBs could provide an important contribution to the asymmetry between warm and cold events.

5. Conclusions

We examine the role of westerly wind burst (WWB) modulation by the large-scale SST, and hence by ENSO

itself, while introducing three new elements. First, we allow the WWBs to be partially stochastic; second, we use a hybrid coupled model of an ocean GCM coupled to a statistical atmosphere rather than the intermediate complexity models used in earlier studies (Eisenman et al. 2005; Perez et al. 2005); finally, we allow for WWBs that move eastward with the warm-pool edge during the development of a warm event.

We find that the modulation of WWBs by the SST leads to the enhancement of the slow interannual component of these winds, which is the component that drives ENSO (Roulston and Neelin 2000; Eisenman et al. 2005). We consequently find that this modulation leads to a significant enhancement of the amplitude of ENSO relative to the case of purely stochastic WWBs. Clearly an ENSO model can always be tuned to reproduce the observed ENSO amplitude by increasing the ocean-atmosphere coupling strength and making the model nearly self-sustained. But given our findings—namely, that modulation of WWBs affects the observed skewness, amplitude, frequency, eastward propagation, number of bursts per year, and seasonal locking of both the bursts and ENSO in this simple framework—we suggest that WWB modulation is likely to play an important role in the dynamics of ENSO. We also find that the movement of the WWBs with the warm-pool edge seems to be playing a possibly important role in further amplifying the developing warm events, suggesting that this migration should be incorporated into any WWB parameterization used in models that do not produce the WWBs as part of the inherent atmospheric dynamics.

The WWB modulation may alternatively be viewed as multiplicative stochastic forcing (Perez et al. 2005). While this point of view may be correct, it is perhaps more illuminating to emphasize the deterministic aspects of the WWB modulation by the SST. Observa-

tions suggest that, given the right SST pattern, WWBs will occur, and the stochastic element of these events can only have a relatively minor effect on their precise timing and characteristics.

Our findings may have important implications for ENSO's predictability. The view that WWBs are purely stochastic, together with their observed strong influence on the onset of warm events, leads to the conclusion that ENSO's predictability limit may not be very long. However, the observation that WWBs are modulated by the SST and therefore have a strong deterministic element raises the hope that ENSO's predictability time is longer than would be expected otherwise. Using the semistochastic WWB approach or simply using an atmospheric model that realistically produces these events as a function of SST (Vecchi et al. 2006) could be a basis for a useful ensemble prediction approach for ENSO. An important consequence of the semistochastic formulation of WWBs presented here is that an ensemble of the coupled system can be easily calculated. For example, the semistochastic component of the WWBs can be recomputed many times for a single set of initial conditions and the spread of trajectories can quantify the effect of WWBs on predictability.

Although we use an ocean general circulation model, the WWB representation used here is clearly idealized. There is only so much that can be learned about the interaction of WWBs and ENSO in a model that does not resolve the relevant physical processes. The next phase of study could involve at least two new aspects. One, the study of ensemble prediction using semistochastic WWBs could quantify the impact of WWBs on predictability. Two, a more accurate determination of the dependence between SST and WWBs based on observations, rather than the overly idealized dependence on the location of the warm-pool edge, may improve the skill of the model (Tziperman and Yu 2007). Finally and most importantly, it would be useful to understand the physical mechanism of WWB modulation by the SST. This last part is clearly very challenging given the complexity of the many different processes leading to the formation of WWBs, and given that many of these processes involve complex interaction with tropical atmospheric convection.

Acknowledgments. We thank Eli Galanti, Gabriel Vecchi, Mojib Latif, Fei-Fei Jin, Gerrit Burgers, Matt Harrison, Shaoqing Zhang, and Tony Rosati for helpful discussions. Three anonymous reviewers greatly improved the presentation. GG, IE, and ET are supported by NSF Climate Dynamics program, grant ATM-0351123, the Geophysical Fluid Dynamics Laboratory, and the McDonnell Foundation. IE is also partially sup-

ported by a NASA Earth System Science Fellowship. ERA-40 data used in this study have been obtained from the ECMWF data server. The calculations of this study were carried out on the Harvard Crimson Grid and the "Swell" Linux cluster at Harvard. Thanks to Chris Walker for computational support.

REFERENCES

- Batstone, C., and H. H. Hendon, 2005: Characteristics of stochastic variability associated with ENSO and the role of the MJO. *J. Climate*, **18**, 1773–1789.
- Battisti, D. S., 1988: Dynamics and thermodynamics of a warming event in a coupled tropical atmosphere–ocean model. *J. Atmos. Sci.*, **45**, 2889–2919.
- , and E. S. Sarachik, 1995: Understanding and predicting ENSO. *Rev. Geophys.*, **33**, 1367–1376.
- Bretherton, C. S., C. Smith, and J. M. Wallace, 1992: An inter-comparison of methods for finding coupled patterns in climate data. *J. Climate*, **5**, 541–560.
- Delcroix, T., G. Eldin, M. McPhaden, and A. Morlière, 1993: Effects of westerly wind bursts upon the western equatorial Pacific Ocean, February–April 1991. *J. Geophys. Res.*, **98** (C9), 16 379–16 385.
- Eisenman, I., L. S. Yu, and E. Tziperman, 2005: Westerly wind bursts: ENSO's tail rather than the dog? *J. Climate*, **18**, 5224–5238.
- Gent, P. R., and J. C. McWilliams, 1990: Isopycnal mixing in ocean circulation models. *J. Phys. Oceanogr.*, **20**, 150–155.
- Griffies, S. M., R. C. Pacanowski, M. Schmidt, and V. Balaji, 2001: Tracer conservation with an explicit free surface method for z-coordinate ocean models. *Mon. Wea. Rev.*, **129**, 1081–1098.
- , M. J. Harrison, R. C. Pacanowski, and A. Rosati, 2003: A technical guide to MOM4. GFDL Ocean Group Tech. Rep. 5. [Available online at http://www.gfdl.noaa.gov/~smg/pointers/geo_physics_abstracts/guide.pdf.]
- Harrison, D. E., and P. S. Schopf, 1984: Kelvin-wave-induced anomalous advection and the onset of surface warming in El Niño event. *Mon. Wea. Rev.*, **112**, 923–933.
- , and B. Giese, 1988: Remote westerly wind forcing of the eastern equatorial Pacific; Some model results. *Geophys. Res. Lett.*, **15**, 804–807.
- , and G. A. Vecchi, 1997: Westerly wind events in the tropical Pacific, 1986–95. *J. Climate*, **10**, 3131–3156.
- , and —, 1999: On the termination of El Niño. *Geophys. Res. Lett.*, **26**, 1593–1596.
- Harrison, M. J., A. Rosati, B. J. Soden, E. Galanti, and E. Tziperman, 2002: An evaluation of air–sea flux products for ENSO simulation and prediction. *Mon. Wea. Rev.*, **130**, 723–732.
- Jin, F.-F., D. Neelin, and M. Ghil, 1994: El Niño on the devil's staircase: Annual subharmonic steps to chaos. *Science*, **264**, 70–72.
- Kerr, R. A., 1999: Atmospheric science: Does a globe-girdling disturbance jigger El Niño? *Science*, **285**, 322–323.
- Kessler, W. S., and R. Kleeman, 2000: Rectification of the Madden–Julian oscillation into the ENSO cycle. *J. Climate*, **13**, 3560–3575.
- , M. J. McPhaden, and K. M. Weickmann, 1995: Forcing of intraseasonal Kelvin waves in the equatorial Pacific. *J. Geophys. Res.*, **100** (C6), 10 613–10 631.
- Kleeman, R., and A. M. Moore, 1997: A theory for the limitation of ENSO predictability due to stochastic atmospheric transients. *J. Atmos. Sci.*, **54**, 753–767.

- Large, W., J. C. McWilliams, and S. C. Doney, 1994: Oceanic vertical mixing: A review and model with nonlocal boundary layer parameterization. *Rev. Geophys.*, **32**, 363–403.
- Latif, M., J. Biercamp, and H. von Storch, 1988: The response of a coupled ocean–atmosphere general circulation model to wind bursts. *J. Atmos. Sci.*, **45**, 964–979.
- Lengaigne, M., E. Guilyardi, J. P. Boulanger, C. Menkes, P. Delecluse, P. Inness, J. Cole, and J. Slingo, 2004: Triggering of El Niño by westerly wind events in a coupled general circulation model. *Climate Dyn.*, **23**, 601–620.
- McPhaden, M. J., 2004: Evolution of the 2002/03 El Niño. *Bull. Amer. Meteor. Soc.*, **85**, 677–695.
- Neelin, J. D., 1990: A hybrid coupled general circulation model for El Niño studies. *J. Atmos. Sci.*, **47**, 674–693.
- Penland, C., and P. D. Sardeshmukh, 1995: The optimal growth of tropical sea surface temperature anomalies. *J. Climate*, **8**, 1999–2024.
- Perez, C. L., A. M. Moore, J. Zavala-Garay, and R. Kleeman, 2005: A comparison of the influence of additive and multiplicative stochastic forcing on a coupled model of ENSO. *J. Climate*, **18**, 5066–5085.
- Picaut, J., F. Masia, and Y. DuPenhoat, 1997: An advective-reflective conceptual model for the oscillatory nature of the ENSO. *Science*, **277**, 663–666.
- Roulston, M. S., and J. D. Neelin, 2000: The response of an ENSO model to climate noise, weather noise and intraseasonal forcing. *Geophys. Res. Lett.*, **27**, 3723–3726.
- Sweeney, C., A. Gnanadesikan, S. M. Griffies, M. J. Harrison, A. J. Rosati, and B. L. Samuels, 2005: Impacts of shortwave penetration depth on large-scale ocean circulation and heat transport. *J. Phys. Oceanogr.*, **35**, 1103–1119.
- Tziperman, E., and L. Yu, 2007: Quantifying the dependence of westerly wind bursts on the large-scale tropical Pacific SST. *J. Climate*, **20**, 2760–2768.
- , L. Stone, M. A. Cane, and H. Jarosh, 1994: El Niño chaos: Overlapping of resonances between the seasonal cycle and the Pacific Ocean–atmosphere oscillator. *Science*, **264**, 72–74.
- , M. A. Cane, and S. E. Zebiak, 1995: Irregularity and locking to the seasonal cycle in an ENSO prediction model as explained by the quasi-periodicity route to chaos. *J. Atmos. Sci.*, **52**, 293–306.
- Vecchi, G. A., and D. E. Harrison, 2000: Tropical Pacific sea surface temperature anomalies, El Niño, and equatorial westerly wind events. *J. Climate*, **13**, 1814–1830.
- , A. T. Wittenberg, and A. Rosati, 2006: Reassessing the role of stochastic forcing in the 1997–1998 El Niño. *Geophys. Res. Lett.*, **33**, L01706, doi:10.1029/2005GL024738.
- Verbickas, S., 1998: Westerly wind bursts in the tropical Pacific. *Weather*, **53**, 282–284.
- Wittenberg, A. T., 2002: ENSO response to altered climates. Ph.D. thesis, Princeton University, 475 pp.
- Yu, L., R. A. Weller, and W. T. Liu, 2003: Case analysis of a role of ENSO in regulating the generation of westerly wind bursts in the western equatorial Pacific. *J. Geophys. Res.*, **108**, 3128, doi:10.1029/2002JC001498.
- Zebiak, S. E., and M. A. Cane, 1987: A model El Niño–Southern Oscillation. *Mon. Wea. Rev.*, **115**, 2262–2278.
- Zhang, S., M. J. Harrison, A. T. Wittenberg, A. Rosati, J. L. Anderson, and V. Balaji, 2005: Initialization of an ENSO forecast system using a parallelized ensemble filter. *Mon. Wea. Rev.*, **133**, 3176–3201.